© JUL 2026 | IRE Journals | Volume 10 Issue 1 | ISSN: 2456-8880
DOI: https://doi.org/10.64388/IREV10I1-1720104

Reduction of Harmonic Distortion in Synchronous Machines Using a Hybrid Active Filter and ANFIS Technique

UJU I. U[1], EFOKE M. U[2], OBINWA C. I[3], OKAFOR M. E[4], ANYANOR K. I[5], BOB D. M. A[6]
[1, 2, 3, 4, 5]*Department of Electrical/Electronic Engineering, Chukwuemeka Odumegwu Ojukwu University, Uli. Anambra State, Nigeria.*
[6]*Ken Saro Wiwa Polytechnic, Bori, Rivers State, Nigeria*

Abstract- Harmonic distortion generated by nonlinear loads poses a significant threat to the performance and operational reliability of synchronous machines by degrading waveform quality, increasing electrical losses, and reducing machine efficiency. This study investigates the effectiveness of a standalone active filter and a hybrid Active Filter–Adaptive Neuro-Fuzzy Inference System (Filter/ANFIS) in mitigating harmonic distortion in a synchronous machine at the Ibom Power Plant. Mathematical models of the synchronous machine and filtering schemes were developed and implemented in MATLAB/Simulink. Performance evaluation was conducted under no-load (0 MW) and full-load (20 MW) operating conditions using Total Harmonic Distortion (THD) as the evaluation metric. At 20 MW, the unfiltered system recorded THD values of 20.00% for current, 18.92% for voltage, and 18.20% for frequency, confirming the significant deterioration in power quality under increased loading. In contrast, waveform ripples observed at 0 MW indicated the presence of inherent harmonic distortion even under no-load operation. The standalone active filter reduced the current THD from 20.00% to 5.12%, while the proposed Filter/ANFIS hybrid further reduced it to 4.13%, demonstrating superior harmonic suppression through adaptive neuro-fuzzy control. The results establish that integrating ANFIS with an active filter significantly enhances harmonic mitigation and improves waveform quality, thereby increasing the operational stability, efficiency, and power quality of synchronous machines. The proposed hybrid technique provides a robust and intelligent solution for harmonic distortion reduction in modern power generation systems.

Keywords: Harmonic Distortion, Synchronous Machine, Active Filter, ANFIS, Hybrid Filtering, Power Quality.

I. INTRODUCTION

The rapid expansion of industrial automation, renewable energy integration, power electronic converters, adjustable-speed drives, and other nonlinear electrical loads has significantly increased harmonic pollution in modern power systems. Harmonic distortion has become a major power quality concern because it adversely affects the performance, efficiency, and reliability of electrical equipment. Synchronous machines are particularly vulnerable to harmonic distortion, which increases losses, overheating, torque pulsations, vibration, insulation deterioration, and reduces machine lifespan. Consequently, maintaining acceptable harmonic levels has become essential for improving power quality and ensuring reliable operation of modern electrical power systems.

Numerous studies have investigated harmonic mitigation and power quality improvement. Efoke et al. (2026) demonstrated that hybrid harmonic mitigation techniques effectively reduce Total Harmonic Distortion (THD), improve waveform quality, and enhance the operational efficiency of synchronous machines. Likewise, Atuchukwu et al. (2021) reported that finite impulse response digital filters significantly suppress harmonic components. However, these approaches rely on fixed controller parameters and therefore perform less effectively under dynamic operatingconditions.

Recent advances in artificial intelligence have introduced intelligent control techniques capable of overcoming many limitations of conventional controllers. Asanya et al. (2023) employed a neuro-fuzzy excitation controller to enhance rotor angle stability, while Okoro et al. (2025) applied Artificial Neural Networks for fault detection and mitigation in synchronous generators. Uju et al. (2024) demonstrated that vector control improves speed regulation, torque response and current regulation, whereas Otor et al. (2024) showed that integrating vector control with Model Predictive Control further enhances transient response and machine efficiency. Although these approaches improve machine performance, they do not directly address adaptive harmonic suppression.

Several researchers have also concentrated on improving power system stability and operational efficiency through advanced control and optimization techniques. Uju et al. (2021) demonstrated that optimized PID controllers improve transient stability and voltage regulation, whereas Uju and Nwadike (2020) showed that optimal placement of FACTS devices enhances voltage stability, reactive power compensation and transmission capability. Atuchukwu et al. (2021) improved Automatic Voltage Regulator performance, resulting in better transient stability. Chijioke et al. (2019), Bright et al. (2019a, 2019b), and Obinwa and Chidolue (2014) established that reactive power compensation and Primal-Dual Interior-Point load flow optimization significantly improve voltage profiles, reduce transmission losses and enhance network stability. Expanding on this work, Obinwa, Nwabueze, and Mbachu (2020) optimized a single control variable using the PD-IP technique and achieved improved voltage regulation, lower real and reactive power losses, faster convergence and enhanced generation utilization. Obinwa (2020a) further demonstrated that simultaneous optimization of two control variables produced superior voltage regulation, improved reactive power distribution, enhanced transmission capability and greater operational efficiency than single-variable optimization. Collectively, these studies demonstrate that advanced optimization techniques substantially improve transmission system performance but do not explicitly consider harmonic distortion or Total Harmonic Distortion.

A comparative assessment of the literature reveals that conventional filters reduce harmonics but lack adaptability, whereas intelligent controllers improve stability, efficiency and reliability without integrating adaptive harmonic compensation. Existing studies have therefore treated harmonic filtering, intelligent control and system optimization as separate research domains. This reveals an important research gap requiring an integrated intelligent harmonic mitigation framework.

The Adaptive Neuro-Fuzzy Inference System (ANFIS), which combines neural learning with fuzzy reasoning, provides an effective platform for adaptive nonlinear control. When integrated with a Hybrid Active Power Filter (HAPF), ANFIS can continuously optimize filter parameters in real time, thereby improving harmonic compensation accuracy, reducing THD, enhancing voltage and current waveform quality, minimizing electrical losses, and improving the efficiency, stability and reliability of synchronous machines. Accordingly, this study proposes a Hybrid Active Filter integrated with ANFIS for adaptive harmonic mitigation in synchronous machines to improve power quality under varying operating conditions.

II. METHODS

2.1 Research Procedure

This study adopted a simulation-based methodology to investigate the effectiveness of a hybrid active power filter (HAPF) integrated with an adaptive neuro-fuzzy inference system (ANFIS) for mitigating harmonic distortion in a synchronous generating plant. The methodology focused on Ibom power station as the case study because of the availability of reliable operational data. MATLAB/Simulink served as the primary software environment for system modeling, controller development, harmonic analysis, and performance evaluation.

The materials utilized in the study included the operational data sheet of the Ibom synchronous generating unit, MATLAB/Simulink software for mathematical modeling and simulation, the ANFIS toolbox for intelligent controller development, Microsoft Excel for organizing and preprocessing simulation data, Microsoft Word for documentation, and an HP laptop for executing the simulations.

The research commenced with the collection of generator and transmission system data from the National Control Centre (NCC), Osogbo. The acquired data included generator rating, terminal voltage, stator current, operating frequency, transformer parameters, transmission line

© JUL 2026 | IRE Journals | Volume 10 Issue 1 | ISSN: 2456-8880
DOI: https://doi.org/10.64388/IREV10I1-1720104

characteristics, and loading conditions. These parameters were used to develop a mathematical model of the Ibom synchronous generating plant and its associated transmission network.

The mathematical model was implemented in MATLAB/Simulink to represent the normal operating condition of the synchronous generator. Harmonic-producing nonlinear loads were then introduced into the network to simulate practical operating conditions and evaluate their impact on generator performance. The study focused on three principal performance parameters, namely terminal voltage, stator current, and operating frequency, because these parameters provide reliable indicators of harmonic effects on synchronous machines. Fast Fourier Transform (FFT) analysis was applied to the voltage and current waveforms to determine the harmonic spectrum and calculate the corresponding Total Harmonic Distortion (THD) under harmonic-distorted conditions.
Following the harmonic assessment, a hybrid active power filter (HAPF) was designed and integrated into the simulated power system to compensate for harmonic currents generated by the nonlinear loads. To enhance the adaptive performance of the filter under varying operating conditions, an adaptive neuro-fuzzy inference system (ANFIS) controller was developed and incorporated into the active filtering unit. The ANFIS controller was trained using simulation data generated from different loading conditions to enable it to learn the nonlinear characteristics of the system and produce optimal compensating signals for effective harmonic suppression.

The proposed hybrid active filter /ANFIS model was subsequently simulated under two loading conditions of 0 MW (no-load) and 20 MW (full-load) to evaluate its effectiveness in mitigating harmonic distortion. The performance of the system before and after implementing the proposed technique was assessed by comparing the voltage, current, and frequency responses together with the corresponding voltage and current Total Harmonic Distortion (THD). The obtained results were further evaluated against the harmonic limits specified in IEEE Standard 519 to determine the level of harmonic mitigation achieved by the proposed intelligent filtering approach.

Finally, MATLAB M-files and the command window were employed for numerical computation, FFT-based harmonic analysis, and graphical presentation of the simulation results. The effectiveness of the proposed Hybrid Active Filter integrated with ANFIS was established through reductions in voltage and current harmonic distortion, improved waveform quality, and enhanced frequency stability of the Ibom synchronous generating plant. The overall research procedure, from data acquisition through mathematical modeling, HAPF-ANFIS implementation, simulation, and performance evaluation, is summarized in the flowchart presented in Figure 1.

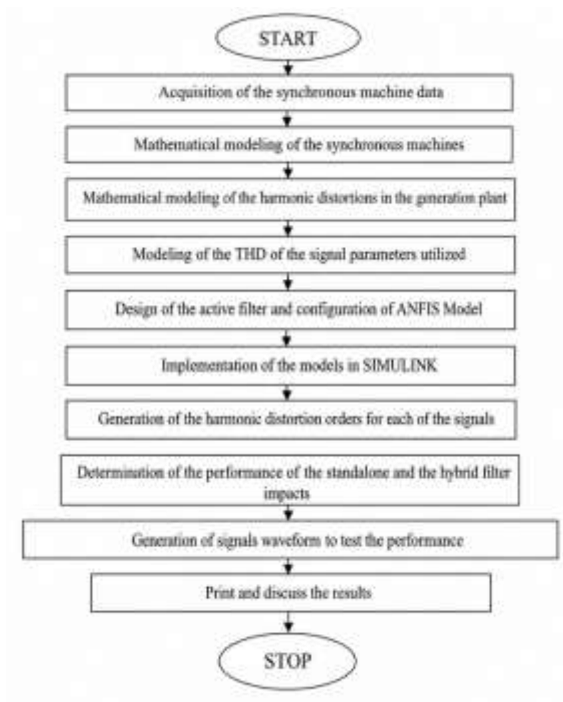

Figure 1; Flow diagram of the Research procedure.

2.2. Data Acquisition.
In the 18 generation stations that are existent in the Nigerian power system network, it was found that Ibom Power plant utilized synchronous machine.

The data for the Ibom steam power plant was shown in table 1

Table 1: Data for Ibom power plant

Parameters (units)	Values
Voltage (kV)	15
Speed (rpm)	299

© JUL 2026 | IRE Journals | Volume 10 Issue 1 | ISSN: 2456-8880
DOI: https://doi.org/10.64388/IREV10I1-1720104

Inertia (Kgm^2)	22
Temperature tolerance (C)	50
Power rating (MW)	60
Resistance (Ohm)	0.024
Impedance (Ohm)	0.0117
Reactance (Ohms)	0.0413
Inductance (H)	0.0332
Frequency (Hz)	50

2.2.1 Mathematical Modeling of the Synchronous Machine

The type of synchronous machine installed in the generation station is permanent magnet brushless synchronous machines. The modeling of the synchronous machine commenced from Newton's second law where

$$F_o = M_a \frac{dV}{dt} \qquad V = \frac{dx}{dt} \qquad (1)$$

Where Fo represents the force, Ma represents the mass and $\frac{dx}{dt}$ represents the velocity and t being time.

Since the synchronous machine is a rotational system;

$$T = J\frac{d\omega}{dt} \qquad \omega = \frac{d\delta}{dt}$$

(2)

Where T represents torque, $\frac{d\omega}{dt}$ represents moment of inertia, ω represents the angular velocity and δ represents the rotor phase angle.

Based on Ohm's law, Faraday's law and Newton's second law and Kirchhoff's voltage, the output voltage becomes

$$V_{out} = IR + \frac{d\gamma}{dt}$$

(3)

Where V_{out} represents output Voltage, R represents the resistance and $\frac{d\gamma}{dt}$ represents the shaft phase angle.

For the power output (Pout); equation 3 becomes;

$$P_{out} = I^2R + I\frac{d\gamma}{dt}$$

(4)

Hence, the mechanical equations become;

$$J\,0.5P_{out}\frac{d\omega}{dt} = T_m + T_{ee} - T_{fw}$$

(5)

Where T_m, T_{ee},T_{fw} represents the mechanical, electrical and friction windage.

Since the emphasis was on design of brushless synchronous machine, the emphasis was on the T_m and T_{ee}. Hence, equation 5 becomes;

$$J\,0.5P_{out}\frac{d\omega}{dt} = T_m + T_{ee}$$

(6)

Considering no losses in the electrical, T_{ee} becomes;

$$T_{ee} = -\frac{3}{4}P_{out}(\gamma_d I_q - \gamma_q I_d)$$

(7)

Where d and q represents direct and quadrature phase respectively.

Substituting Equation 7 to 6 gives;

$$J\,0.5P_{out}\frac{d\omega}{dt} = T_m - \frac{3}{4}P_{out}(\gamma_d I_q - \gamma_q I_d)$$

(8)

Re-writing equation 8 gives;

$$T_m = J\,0.5P_{out}\frac{d\omega}{dt} + \frac{3}{4}P_{out}(\gamma_d I_q - \gamma_q I_d)$$

(9)

Then, the rotor phase angle becomes;

$$\frac{\Delta\delta}{dt} = \frac{P_{out}}{2}\theta_{sh} - \omega_s t \qquad (10)$$

Where θ_{sh} represents the shaft angle and $\omega_s$represents the speed of the synchronous generator

The circuit diagram of the three-phase circuit diagram of a brushless synchronous machine was shown in figure.2.

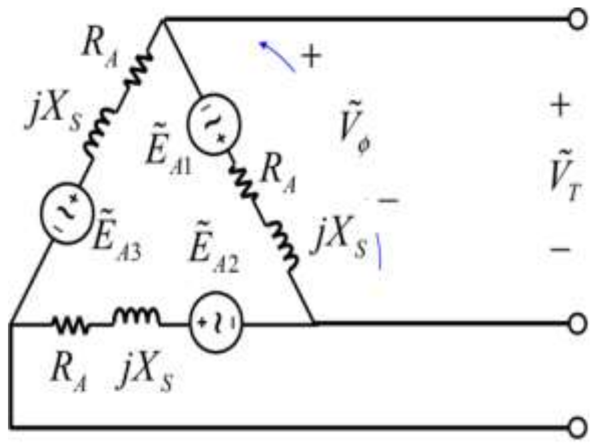

Figure 2. Circuit diagram of 3-phase brushless synchronous machine.

From figure 2, E_{As} represents the three phase internally generated voltages, R represents the resistance, X_s represents the reactance, $V_\emptyset$ represents the phase voltage and V_T = V_{out} represent the output voltage.

The frequency of the synchronous machine f was shown in equation 11.

DOI: https://doi.org/10.64388/IREV10I1-1720104

$$f = \frac{\omega_s P_{ol}}{120} \quad (11)$$

Where P_{ol} represents the number of poles and ω_s represents the speed of the machine.

Hence, the internal voltage of the machine was shown in equation 12.

$$E_{AS} = 1.33 f N \emptyset \quad (12)$$

Where N represents the factor value of the machine construction (for Jebba hydro plant was 15.2217) and $\emptyset$ represents the flux.At a unity power factor, the relationship between the internal voltage E_{AS} and the output voltage V_{out} was shown in equation 13.

$$V_{out} = E_{AS} - XI - RI \quad (13)$$

Where X represent the reactance and R represents the resistance.

Re-arranging equation 13 gives;

$$I = -\frac{V_{out} - E_{AS}}{X - R} \quad (14)$$

Equation 17 represents the output current from the synchronous machine.

The power output for the 3-phase synchronous machine with the phase angle was shown in equation 12.

$$P_{out} = 1.442 V_{out} I \cos\theta \quad (15)$$

Where θ represents the phase angle.

Re-arranging equation 15 gives;

$$\theta = \cos^{-1} \frac{P_{out}}{1.442 V_{out} I} \quad (16)$$

Hence equations 3, 11 and 14, represents voltage, frequency and current signal respectively that was utilized to measure the healthy and impact of the harmonic distorted signals in the synchronous machine.

The developed Simulink block model of the synchronous machine was shown in figure 3

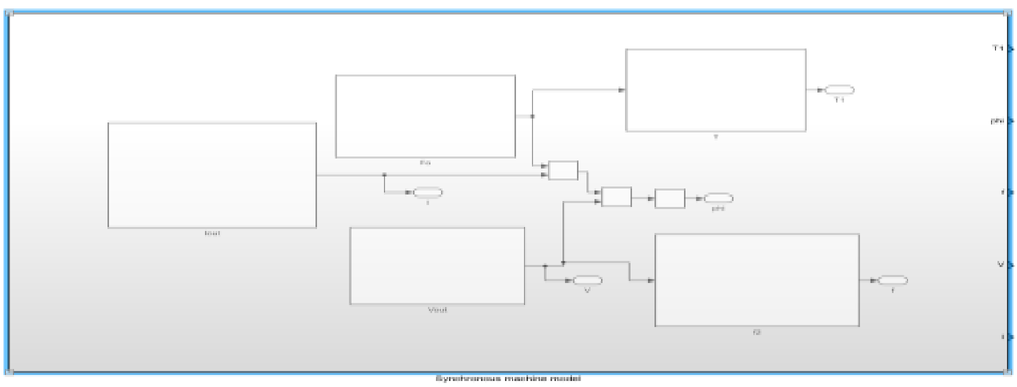

Figure 3: SIMULINK model of the synchronous machine.

The sub system model of the synchronous machine in figure 3 was shown in figure 4

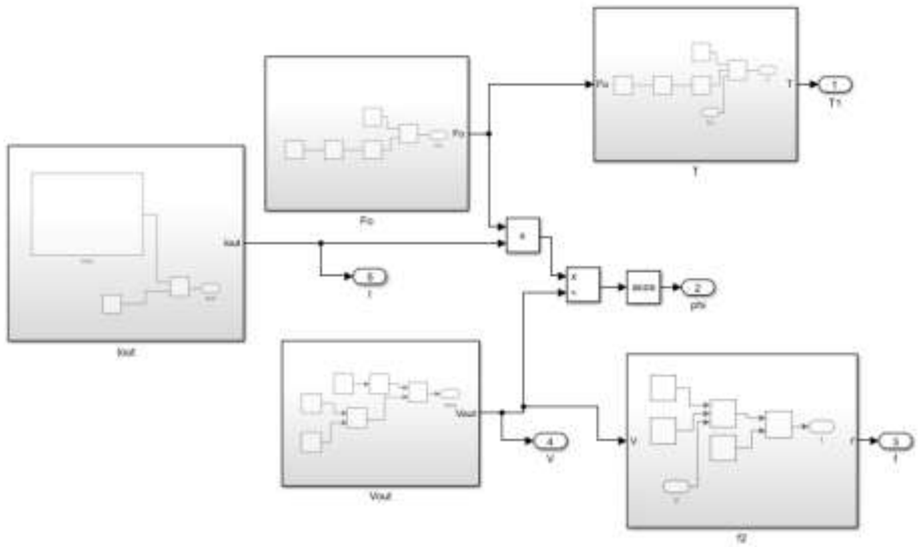

Figure 4: Subsystem model of the synchronous machine

The SIMULINK model of the synchronous machine connected to the load was shown in figure 5

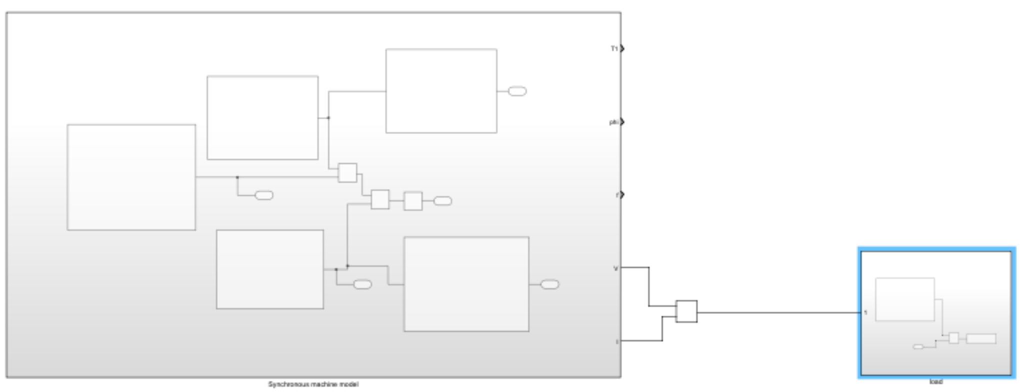

Figure 5: SIMULINK model of the synchronous machine connected to a load

3.2.2 Determination of the THD for each measurement signal

The THD of the voltage signal was obtained using the equation presented below;

$$V_{THD} = (V_{out1} + V_{out2} + V_{out3} + \dots + V_{outn})^{0.5} \quad (17)$$

Where V_{THD} represents the THD of the voltage signal and n represents the harmonics order of the voltage signals.

The THD of the current signal was obtained using the equation presented below;

$$I_{THD} = (I_{out1} + I_{out2} + I_{out3} + \dots + I_{outn})^{0.5} \quad (18)$$

Where I_{THD} represents the THD of the current signal and n represents the harmonics order of the current signals.

The THD of the frequency signal was obtained using the equation presented below;

$$f_{THD} = (f_1 + f_2 + f_3 + \dots + f_n)^{0.5} \quad (19)$$

Where f_{THD} represents the THD of the frequency signal and n represents the harmonics order of the frequency signals.

The THD of the phase angle was obtained using the equation presented below;

$$\theta_{THD} = (\theta_1 + \theta_2 + \theta_3 + \dots + \theta_n)^{0.5} \quad (20)$$

Where θ_{THD} represents the THD of the phase angle and n represents the harmonics order of the phase angle.

The THD of the torque was obtained using the equation presented below;

$$T_{THD} = (T_1 + T_2 + T_3 + \dots + T_n)^{0.5} \quad (21)$$

Where T_{THD} represents the THD of the torque and n represents the harmonics order of the torque.

The order for each of the signals were presented for the generation stations and the load stations and the THD for each of the signals were obtained and presented and the section outcome (results) was considered as the THD of the system without filters.

The harmonic distortion was caused by the presence of disturbance that stems from the presence of non-linear loads. The impact of non-linear load on the voltage signal of the synchronous machine was shown in equation 25.

$$V_{nL} = V_{out} \frac{P_L}{P_{LL}} \ln\left(\frac{Q_L V_L}{I_L}\right)^{\frac{1}{t}} \quad (22)$$

Where V_{nL} represents the harmonic distorted voltage signal, P_L represents the active power flow of the load station, P_{LL} represents the active power loss signal from the load station, Q_L reactive power flow from the load station, V_L represents the voltage signal of the load station and I_L represents the current signal.

The impact of non-linear load on the current signal of the synchronous machine was shown in equation 26.

$$I_{nL} = I_{out} \frac{I_L}{Q_{LL}} \ln\left(\frac{P_L P_{LL}}{I_L}\right)^{\frac{1}{t}} f_L \quad (23)$$

Where I_{nL} represents the harmonic distorted voltage signal, P_L represents the active power flow of the load station, P_{LL} represents the active power loss signal from the load station, Q_L reactive power flow from the load station, f_L represents the frequency signal of the load station and I_L represents the current signal.

The impact of non-linear load on the frequency signal of the synchronous machine was shown in equation 27.

$$f_{nL} = f + f_L \ln\left(\frac{P_L V_L}{I_L}\right)^{\frac{1}{t}} \quad (24)$$

Where f_{nL} represents the harmonic distorted frequency signal, P_L represents the active power flow of the load station, P_{LL} represents the active power loss signal from the load station, V_L represents the voltage signal of the load station, I_L represents the current signal, f_L represents the frequency signal of the load station and t represents the time (in hours).

The impact of non-linear load on the torque of the synchronous machine was shown in equation 28.

$$T_{nL} = T + f_L \exp\left(\frac{Q_L Q_{LL}}{I_L}\right)^{\frac{1}{t}} \quad (25)$$

Where T_{nL} represents the harmonic distorted torque, Q_L represents the reactive power flow of the load station, Q_{LL} represents the reactive power loss signal from the load station, V_L represents the voltage signal of the load station, I_L represents the current signal, f_L represents the frequency signal of the load station and t represents the time (in hours).

The impact of non-linear load on the phase angle of the synchronous machine was shown in equation 29.

$$T_{nL} = T + f_L \log\left(\frac{Q_L P_{LL}}{Q_{LL} I_L}\right)^{\frac{1}{t}} \quad (26)$$

Where T_{nL} represents the harmonic distorted phase angle, Q_L represents the reactive power flow of the load station, Q_{LL} represents the reactive power loss signal from the load station, V_L represents the voltage signal of the load station, I_L represents the current signal, f_L represents the frequency signal of the load station and t represents the time (in hours).

3.2.3 Model for the active filter

The type of active filter utilized in the research was the second-order multiple feed back low pass filter and the circuit diagram was shown in figure 6.

© JUL 2026 | IRE Journals | Volume 10 Issue 1 | ISSN: 2456-8880
DOI: https://doi.org/10.64388/IREV10I1-1720104

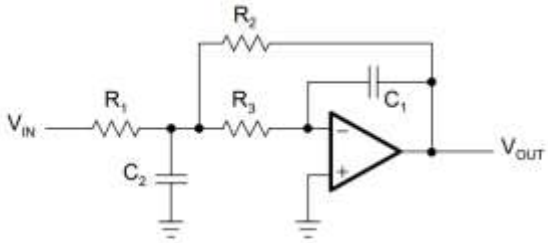

Figure 6: Circuit diagram of the second order active filter

The choice of the filter generally due the multiple feedback nature that was essential in mitigating the THD of the synchronous machines and it is not limited to reducing the voltage harmonic distortion. Study shows that they can be utilized in improving the current signal, frequency signal, torque and the phase of the power plants and power system network. However, the gains must be high for the filter to be effective.

The model for the active filter was presented in transfer function. Hence, the outcome of the measuring signals output (D(s)) was shown in the equation below.

$$D(s) = \frac{D_0}{1+d_1 s+d_2 s^2} \tag{27}$$

Where

$$Do = -\frac{R_2}{R_1} \tag{28}$$

$$d_1 = C_1\left(R_2 + R_3 + \left(\frac{R_2 R_3}{R_1}\right)\right) \tag{29}$$

$$d_2 = C_1 C_2 R_2 R_3 \tag{30}$$

Where R represents the resistance of the resistors and C represents the capacitance of the capacitors.

The Simulink model with the active filter was shown in figure 7

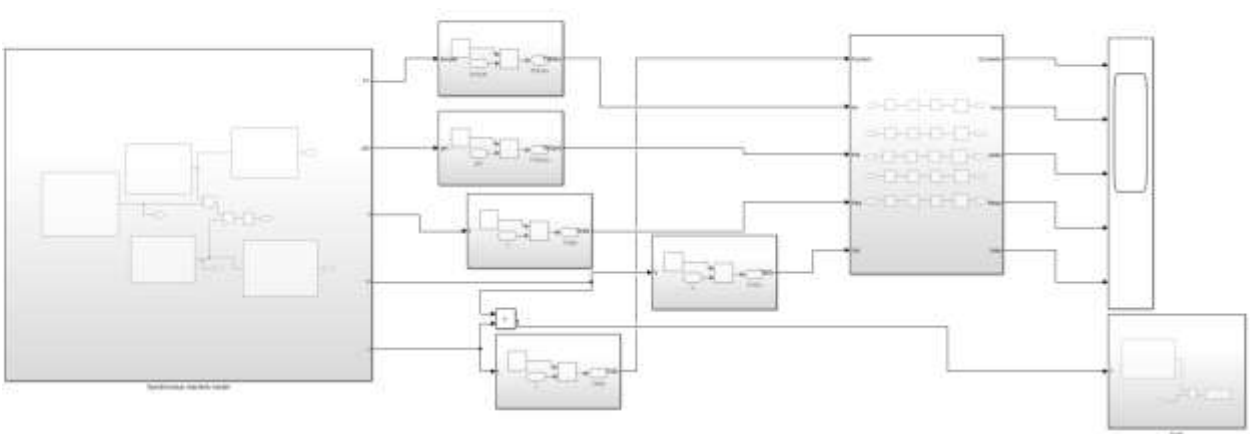

Figure 7: SIMULINK model with active filter

3.2.4 ANFIS model Configuration as a hybrid to the Active filter

The ANFIS was utilized as an hybrid to the active filter to boost the filter performance and reduce the harmonic distortion occurrence in the synchronous machine. The block diagram for the modeling of the ANFIS model in MatLab was shown in figure 8.

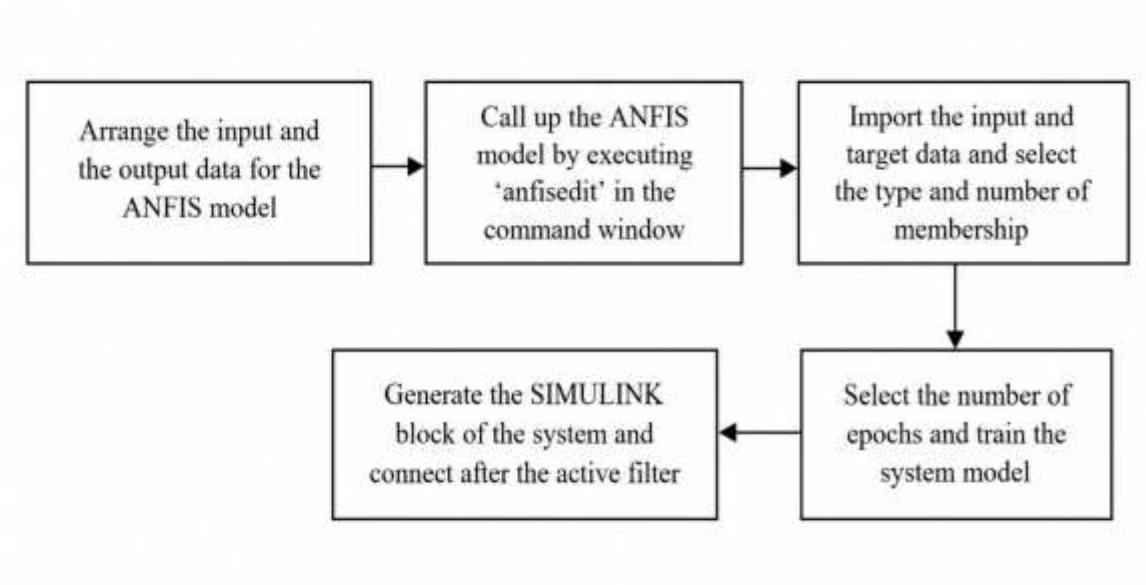

Figure 8: Block diagram of the ANFIS modeling procedure

The inputs to the ANFIS model were the filtered signals from the active filter and the output from the ANFIS signal was a filtered signal for each of the signal parameters with THD less than 2%.

The type of membership function utilized for the input variable was the triangular membership function and the number of membership functions for each input variable was 3. For the output variables, the type of membership function utilized was linear and the number of membership functions was equal to the inference rules in the Model. The type of inference rules implemented was sugeno inference rules.

The Simulink model showing the synchronous machine with the filter/ANFIS control mechanism was shown in figure 9.

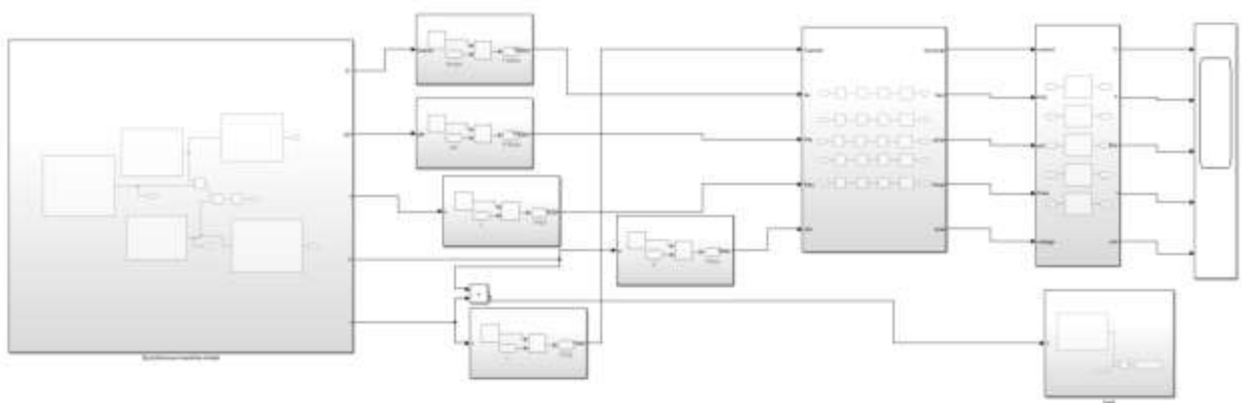

Figure 9: SIMULINK model with filter/ANFIS model

III. RESULTS

The performance of the proposed Hybrid Active Power Filter integrated with ANFIS was evaluated using the voltage, current, and operational frequency responses of the Ibom synchronous generating plant under 0 MW and 20 MW loading conditions. Harmonic mitigation effectiveness was assessed using Total Harmonic Distortion (THD) obtained from Fast Fourier Transform (FFT) analysis before and after filter implementation. The results demonstrate the capability of the proposed approach to reduce

© JUL 2026 | IRE Journals | Volume 10 Issue 1 | ISSN: 2456-8880
DOI: https://doi.org/10.64388/IREV10I1-1720104

harmonic distortion and improve power quality in compliance with IEEE Standard 519.

3.0 Results of harmonic distortion without active filter

3.1 Harmonic distortion Results in Ibom power plant

The current signal at load of 0MW was shown in figure 10.

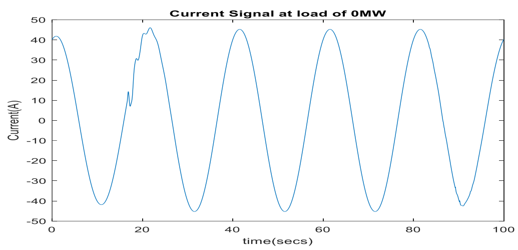

Figure 10: Current signal at 0MW for Ibom Plant without filter.

The current signal at load of 20MW was shown in figure 11.

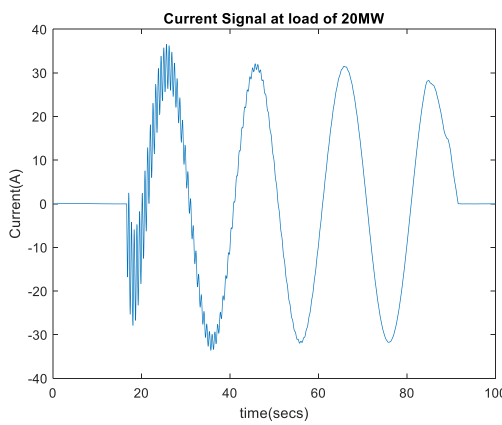

Figure 11: Current signal at 20MW for Ibom Plant without filter

The voltage signal at load of 0MW was shown in figure 12.

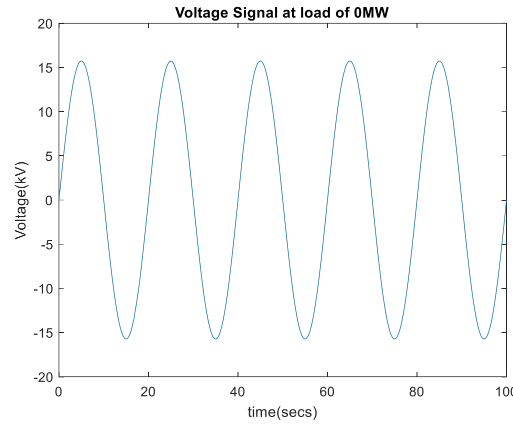

Figure 12: Voltage signal at 0MW for Ibom Plant without filter

The voltage signal at load of 20MW was shown in figure 13.

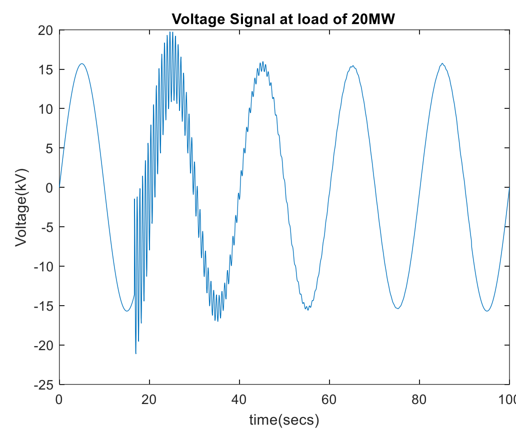

Figure 13: Voltage signal at 20MW for Ibom Plant without filter

The frequency signal at load of 0MW was shown in figure 14.

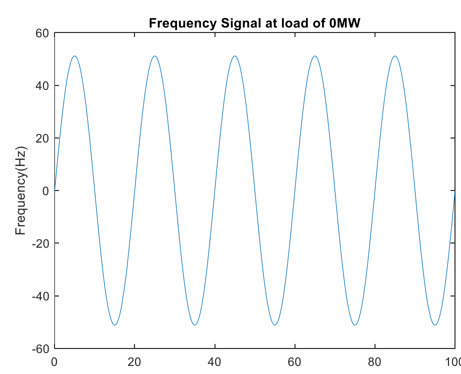

Figure 14: Frequency signal at 0MW for Ibom Plant without filter

The frequency signal at load of 20MW was shown in figure 15.

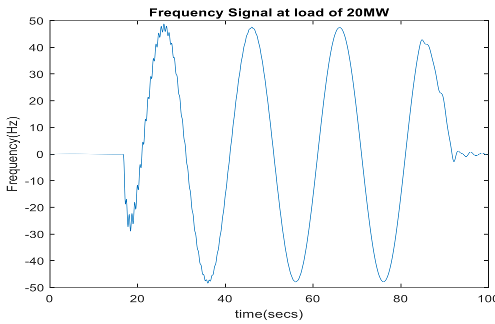

Figure 15: Frequency signal at 20MW for Ibom Plant without filter

3.2 . Results showing the level of harmonic distortion at 0MW and 20MW without filter and after mitigation with the different techniques with active filter/ANFIS

The comparative analysis of the Current signal at 0MW for Ibom Plant was shown in figure 16

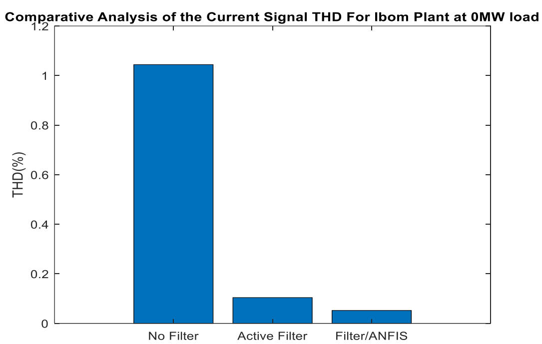

Figure 16: The comparative analysis of the Current signal at 0MW for Ibom Plant

The comparative analysis of the Current signal at 20MW for Ibom Plant was shown in figure 17

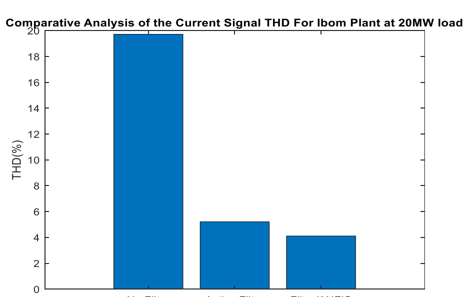

Figure 17. The comparative analysis of the Current signal at 20MW for Ibom Plant

The comparative analysis of the voltage signal at 0MW for Ibom Plant was shown in figure 18

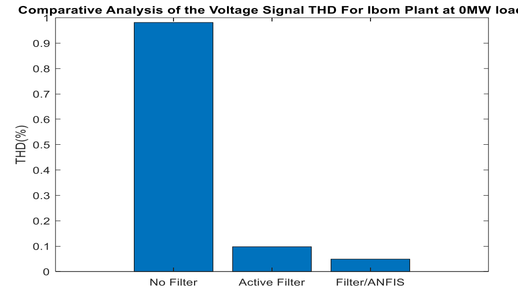

Figure 18. The comparative analysis of the voltage signal at 0MW for Ibom Plant .

The comparative analysis of the voltage signal at 20MW for Ibom Plant was shown in figure 19.

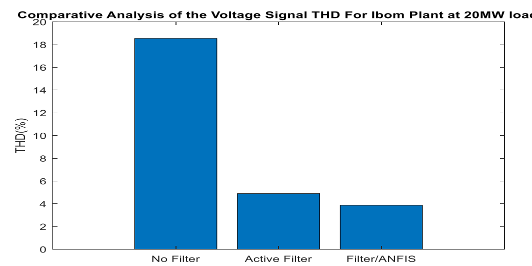

Figure 19. The comparative analysis of the voltage signal at 20MW for Ibom Plant

The comparative analysis of the frequency signal at 0MW for Ibom Plant was shown in figure 20.

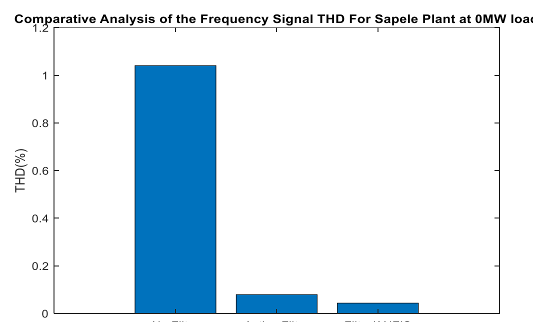

Figure 20. The comparative analysis of the frequency signal at 0MW for Ibom Plant

The comparative analysis of the frequency signal at 20MW for Ibom Plant was shown in figure 21

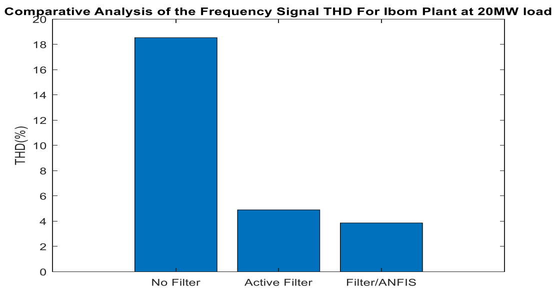

Figure 21. The comparative analysis of the frequency signal at 20MW for Ibom Plant.

IV. DISCUSSION OF RESULTS

The results demonstrated that harmonic distortion significantly affects the performance of synchronous machines and becomes increasingly severe as loading conditions increase. The waveforms presented in Figures 10 to 15 reveal the presence of signal ripples in the current, voltage, and frequency responses at both 0 MW and 20 MW loading conditions before filter implementation. The distortions observed indicate that synchronous machines are susceptible to harmonics generated by nonlinear loads, resulting in degraded power quality and reduced operational stability.

At full load (20 MW), the Total Harmonic Distortion (THD) values obtained without filtering were 20.0%, 18.92%, and 18.20% for the current, voltage, and frequency signals, respectively. These values significantly exceed the 5% harmonic limit recommended by IEEE Standard 519, confirming the adverse effects of harmonic distortion on synchronous machine operation. The increase in waveform ripples observed in Figures 11,13, and 15 further suggests that loading conditions substantially influence harmonic propagation within the power system. The distorted waveforms imply increased machine losses, insulation stress, reduced efficiency, and possible deterioration of machine lifespan under prolonged operation.

The implementation of the active filter considerably improved the harmonic profile of the synchronous machine. For the current signal, the THD value reduced from 20.0% to 5.12%, representing a reduction of approximately 74.4%. Although this performance approached IEEE harmonic limits, slight harmonic components remained evident under varying operating conditions. This observation supports previous findings that conventional filtering techniques provide satisfactory harmonic mitigation but may exhibit limitations in adapting to dynamic system behaviour

The integration of the Adaptive Neuro-Fuzzy Inference System (ANFIS) with the Hybrid Active Power Filter provided superior harmonic suppression performance. The proposed HAPF-ANFIS technique reduced the current signal THD from 20.0% to 4.13%, representing an overall reduction of approximately 79.35%. This significant improvement demonstrates the adaptive capabilities of the intelligent controller in continuously optimizing harmonic compensation under changing loading conditions. The improved waveform characteristics shown in Figures 16 and 17 indicate that the ANFIS controller effectively learns the nonlinear behaviour of the system and generates optimal compensating signals for harmonic mitigation.

Similarly, the voltage and frequency responses illustrated in Figures 18 to 21 exhibited substantial improvements after filter implementation. The reduction in waveform distortions indicates enhanced voltage regulation and improved frequency stability of the synchronous generating plant. Frequency stability is particularly important in interconnected power systems because harmonic-induced frequency disturbances may adversely affect synchronization and protection coordination. Consequently, minimizing harmonic components contributes directly to improved operational reliability and system efficiency.

The results further establish that intelligent filtering techniques provide substantial advantages over conventional harmonic mitigation approaches. By combining active filtering with adaptive neuro-fuzzy reasoning, the proposed technique simultaneously improves waveform quality, reduces electrical losses, and enhances the operational stability of synchronous machines. The THD values achieved satisfy IEEE Standard 519 requirements, demonstrating the suitability of the proposed Hybrid Active Power Filter integrated with ANFIS for real-time harmonic mitigation in modern synchronous generating systems operating under varying loading conditions.

V. CONCLUSION

This study investigated the application of a Hybrid Active Power Filter integrated with an Adaptive Neuro-Fuzzy Inference System (HAPF-ANFIS) for mitigating harmonic distortion in synchronous machines under varying loading conditions. The results established that harmonic distortion significantly degrades the current, voltage, and frequency characteristics of synchronous generating systems, particularly at higher loading conditions. At 20 MW loading, the Total Harmonic Distortion values obtained without filtering were 20.0%, 18.92%, and 18.20% for the current, voltage, and frequency signals, respectively, exceeding the IEEE Standard 519 recommended harmonic limits and indicating substantial power quality deterioration.

The implementation of the conventional active filter reduced the current signal THD to 5.12%, demonstrating the effectiveness of active filtering techniques in harmonic suppression. However, the proposed HAPF-ANFIS model provided superior performance by reducing the current signal THD to 4.13%, representing an 79.35% reduction in harmonic distortion relative to the unfiltered system. The improved waveform characteristics and enhanced frequency stability further demonstrate the adaptive capability of the ANFIS controller in optimizing harmonic compensation under dynamic operating conditions.

The findings of this study establish that integrating intelligent control techniques with active harmonic filtering significantly improves power quality, operational stability, and the reliability of synchronous generating plants. The proposed HAPF-ANFIS framework therefore provides an efficient and adaptive solution for real-time harmonic mitigation and offers significant potential for application in modern power systems characterized by increasing penetration of nonlinear electrical loads and renewable energy technologies.

REFERENCES

[1] Asanya, O. N., Uju, I. U., Abonyi, S. E., & Ozor, G. O. (2023). Enhancing rotor angle stability of synchronous generators using neuro-fuzzy excitation control model. International Journal of Latest Technology in Engineering, Management & Applied Science, 12(4), 233-254.

[2] Atuchukwu, A. J., Uju, I. U., & Awgu, I. M. (2021). Performance enhancement of automatic voltage regulator (AVR) for stability in power generation. Iconic Research and Engineering Journals, 5(6).

[3] Atuchukwu, A. J., Uju, I. U., & Efoke, M. U. (2021). Reduction of harmonics in power lines using finite impulse response filter. Journal of Engineering Research and Reports, 21(12), 18-28.

[4] Bright, G. C. E., Uju, I. U., & Ohia, C. C. (2019). Predicting weak nodes for reactive compensation in Nigeria power network. Iconic Research and Engineering Journals, 2(11).

[5] Bright, G. C. E., Uju, I. U., & Onyedikachi, S. N. (2019). Tracing power system weak nodal shifts following reactive power compensation. International Journal for Research & Development, 7(6).

[6] Chijioke, J., Uju, I. U., & Atuchukwu, A. J. (2019). Automatic power factor correction for variable inductive load industries. Iconic Research and Engineering Journals.

[7] Efoke, M. U., et al. (2026). Reduction of harmonic distortions in synchronous machines using hybrid techniques. International Journal of Advances in Engineering and Management, 8(6), 41-54.

[8] Macmammah, M., Atuchukwu, J., Obinwa, C. I., & Agbaraji, C. E. (2021). Robust compensating function scheme for adequate electrical power system stabilization. Journal of Scientific Research & Reports, 27(4), 80-91.

[9] Obinwa, C. I., & Chidolue, G. C. (2014). Primal-Dual Interior-Point load flow technique for optimisation in 330 kV power system.

[10] Obinwa, C. I., Nwabueze, C. A., & Mbachu, C. B. (2020). Primal-dual interior-point technique for optimisation of 330 kV power system on one

variable. European Journal of Engineering Research and Science, 5(2).

[11] Obinwa, C. I. (2020). Primal-dual interior-point technique for optimisation of 330 kV power system on two variables. World Journal of Engineering Research and Technology, 6(2), 433-451.

[12] Okoro, F., & Uju, I. U. (2024). Synchronous generator protection and generator synchronization in a power system. Global Scientific Journals, 12(12).

[13] Okoro, F., Uju, I. U., Obineche, J. A., & Nwosu, A. W. (2025). Enhancing faults detection and mitigation of synchronous generators using artificial neural network. Global Scientific Journals, 13(11).

[14] Otor, E., Uju, I. U., Nwosu, A. W., & Imo, F. U. (2024). Enhancing permanent magnet synchronous motor performance characteristics using vector control and model predictive control. International Journal of Progressive Research in Engineering, Management and Science, 4(9), 1264-1276.

[15] Uju, I. U., Atuchukwu, A. J., & Ekeopara, O. E. (2021). Power system stability optimization using PID controller. Iconic Research and Engineering Journals, 4(10).

[16] Uju, I. U., & Nwadike, S. U. (2020). Optimization of power system stability using multiple FACTS placement. International Journal of Engineering Science and Computing, 10(12).

[17] Uju, I. U., Otor, E., & Nwosu, A. W. (2024). Investigating the effect of vector control on permanent magnet synchronous motor performance characteristics. International Journal of Engineering Research and Development, 20(11), 1455-1460….